SUPPORTING INFORMATION

Magnetics-Based Approach for Fine-Tuning Afterload in Engineered Heart Tissues

Marita L. Rodriguez,†,‡ Tessa R. Werner,†,‡ Benjamin Becker,†,‡ Thomas Eschenhagen,†,‡ and Marc N. Hirt*,†,‡

†Department of Experimental Pharmacology and Toxicology, University Medical Center Hamburg-Eppendorf, Martinistraße 52, 20246 Hamburg, Germany

‡DZHK (German Center for Cardiovascular Research), Partner site Hamburg/Kiel/Lübeck, 20246 Hamburg, Germany

Number of pages: 8
Number of figures: 5
Number of tables: 2

Supplementary Fig. S1

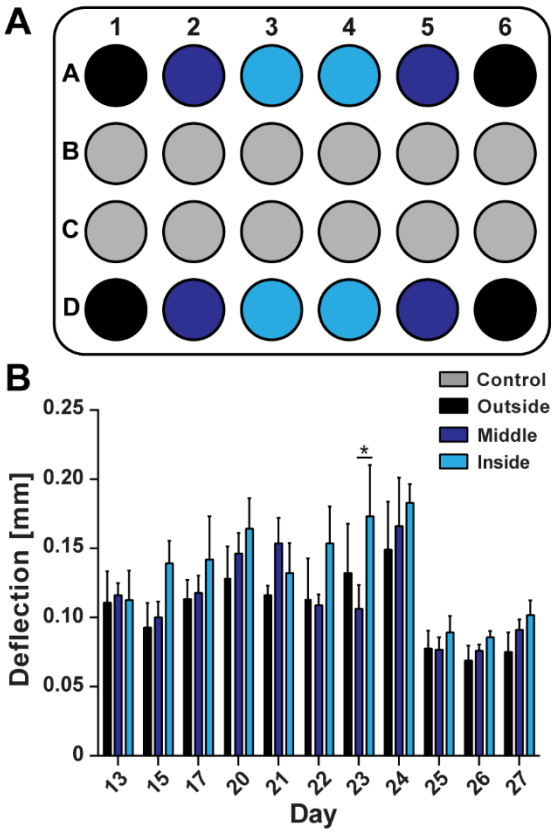

Fig. S1. Uniformity of applied afterload on tissue deflection: The effect of tissue location on post deflection was assessed to determine if there were differences in contractile properties for afterload-affected tissues cultured in the outermost wells versus those in the middle wells or inside wells. (A) A schematic of the 24-well culture plate shows the location of the control (grey), outside (black), middle (dark blue), and inside (light blue) tissues. (B) Over the testing period, there were no differences in tissue deflection with regard to tissue location, with the exception of a measurable difference between inside and middle tissues on day 23. Error bars in graphs represent standard error of the mean. Statistical significance was assessed for n = 12 control tissues and n = 12 afterload-affected tissues at $p < 0.05$, and p-values are graphically displayed as follows: * = $p < 0.05$.

Supplementary Fig. S2

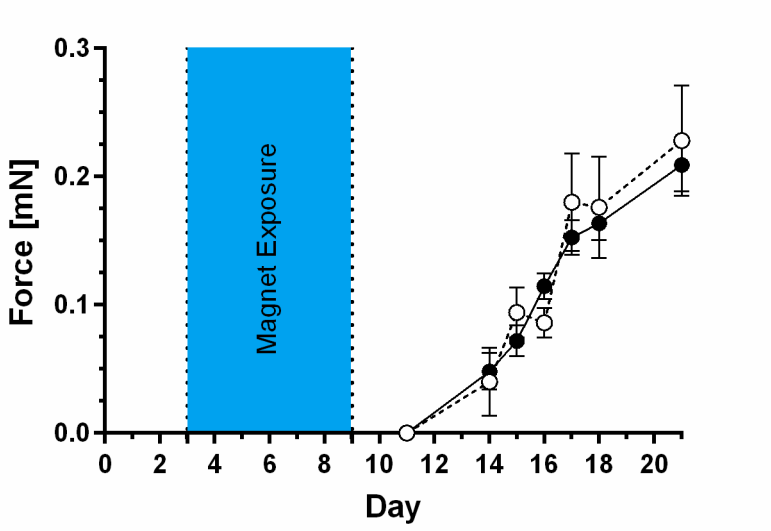

Fig. S2. Effect of long-term magnetic exposure on rEHT contraction: rEHTs were cultured in close proximity to strong permanent magnets to determine any effect of the magnetic fields on the contractile properties of the tissues. Following six days of magnetic field exposure during a critical phase of tissue development (day 3-9), the tissues were monitored for any changes in their contractile forces over the following twelve days. During this time period, no significant differences were found between control tissues (solid circles and lines) and tissues exposed to magnets (open circles and lines). Error bars in graphs represent standard error of the mean. Statistical significance was assessed for n = 11 control tissues and n = 5 magnet exposed tissues at $p < 0.05$.

Supplementary Fig. S3

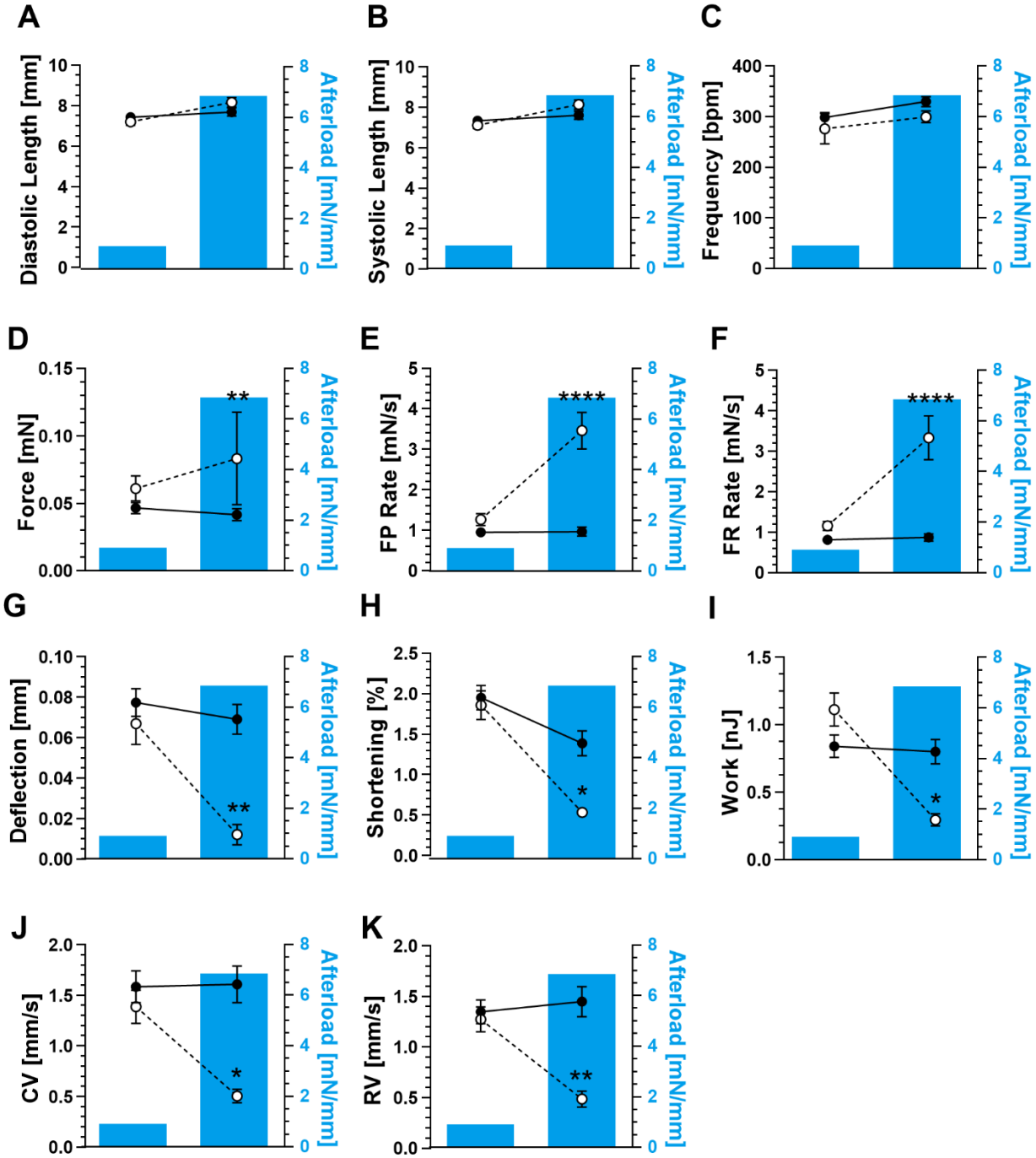

Fig. S3. Contractile properties of rEHTs exposed to a sudden increase in afterload: The effect of a large step-wise increase in afterload on the contractile properties of control (solid line and closed circles) and afterload-affected (dashed line and open circles) rEHTs was assessed by increasing afterload from a baseline value of 0.91 mN/mm to a maximal value of 6.85 mN/mm within a matter of seconds. Immediately following this intervention, there were no significant differences in the average (A) diastolic tissue length, (B) systolic tissue length, or (C) spontaneous beating frequency. Alternatively, despite increases in (D) contractile force, (E) force production rate, and (F) force relaxation rate, average values of (G) post deflection, (H) tissue shortening, (I) work production, (J) contractile velocity, and (K) relaxation velocity all significantly decreased for afterload-affected tissues. Error bars in graphs represent standard error of the mean. Statistical significance was assessed for $n = 12$ control tissues and $n = 4$ afterload-affected tissues at $p < 0.05$, and p-values are graphically displayed as follows: * = $p < 0.05$ and ** = $p < 0.01$.

Supplementary Fig. S4

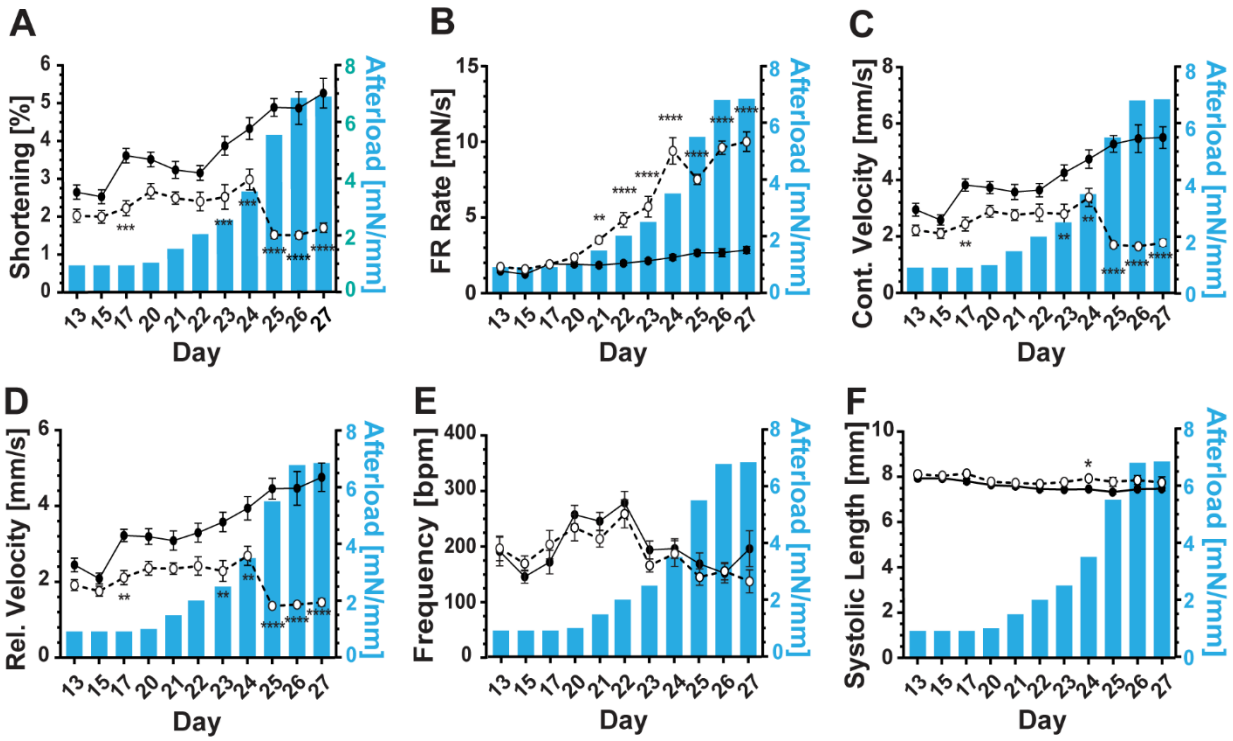

Fig. S4. Supplemental contractile measurements for rEHTs undergoing week long experiment: Contractile measurements of control (solid line and closed circles) and afterload-affected (dashed line and open circles) tissues when increasing tissue load from a stiffness of 0.91 mN/mm to 6.85 mN/mm over a one-week period. Up until day 24, (A) tissue fractional shortening, (B) force relaxation rate, (C) contraction velocity, and (D) relaxation velocity increased over time for both control tissues and afterload-affected tissues. On this day, afterload-affected tissues departed from this trend and demonstrated marked decreases in these contractile properties. Thereafter, a reduction in ΔAL allowed for these properties to partially recover. (E) There were no significant differences in spontaneous beating frequency between control and afterload-affected EHTs over the testing period, and no obvious effect of afterload on frequency. (F) Systolic tissue length remained fairly steady throughout the testing period, and with the exception of day 24, there were no differences in this tissue property between control and afterload-affected tissues. Error bars in graphs represent standard error of the mean. Statistical significance was assessed for n = 12 control tissues and n = 12 afterload-affected tissues at $p < 0.05$, and p-values are graphically displayed as follows: * = $p < 0.05$, ** = $p < 0.01$, *** = $p < 0.001$, **** = $p < 0.0001$.

Supplementary Fig. S5

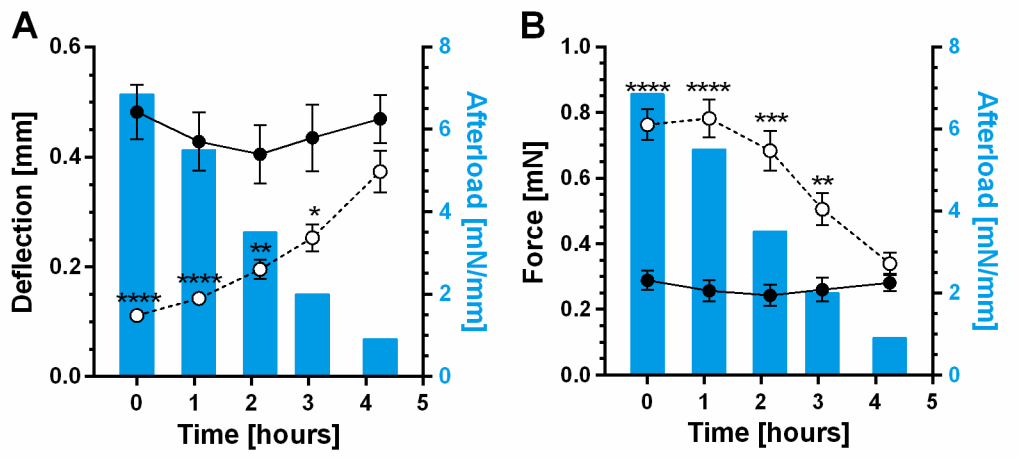

Fig. S5. Contractile response of rEHTs to step-wise decreases in afterload: Measured contractile properties of control (solid line and closed circles) and afterload-affected (dashed line and open circles) tissues exposed to decreasing magnitudes of afterload over a single day. (A) Tissue deflection in control tissues remained relatively constant, while the average post deflection for afterload-affected tissues continually increased with decreasing afterload application. (B) These trends translated into a steady magnitude of contraction for control tissues over the testing period, while those measured for afterload-affected tissues decreased with lower magnitudes of tissue loading. Error bars in graphs represent standard error of the mean. Statistical significance was assessed for n = 9 control tissues and n = 9 afterload-affected tissues at $p < 0.05$, and p-values are graphically displayed as follows: * = $p < 0.05$, ** = $p < 0.01$, *** = $p < 0.001$, **** = $p < 0.0001$.

Supplementary Table S1.

Table. S1. Supplemental contractile data from week long experiment: Average contractile data for control (white) and afterload-affected (grey) tissues for the duration of the testing period. All data is compiled from n = 12 control tissues and n = 12 afterload-affected tissues. Computed error represents the standard error of the mean.

		Day										
Tissue Property	Units	**13**	**15**	**17**	**20**	**21**	**22**	**23**	**24**	**25**	**26**	**27**
Diastolic Length	**[mm]**	7.90 ± 0.10	7.89 ± 0.10	7.85 ± 0.10	7.68 ± 0.09	7.60 ± 0.09	7.47 ± 0.08	7.50 ± 0.07	7.55 ± 0.08	7.47 ± 0.10	7.60 ± 0.08	7.64 ± 0.07
		8.03 ± 0.10	7.96 ± 0.11	8.08 ± 0.09	7.75 ± 0.11	7.68 ± 0.09	7.63 ± 0.08	7.73 ± 0.08	7.85 ± 0.10	7.66 ± 0.19	7.73 ± 0.19	7.64 ± 0.22
Systolic Length	**[mm]**	7.69 ± 0.09	7.69 ± 0.10	7.57 ± 0.10	7.41 ± 0.09	7.35 ± 0.09	7.23 ± 0.09	7.21 ± 0.07	7.23 ± 0.08	7.11 ± 0.09	7.23 ± 0.09	7.24 ± 0.08
		7.87 ± 0.10	7.81 ± 0.11	7.90 ± 0.10	7.54 ± 0.11	7.49 ± 0.08	7.45 ± 0.09	7.54 ± 0.08	7.69 ± 0.10	7.55 ± 0.19	7.62 ± 0.19	7.51 ± 0.22
Deflection	**[mm]**	0.15 ± 0.01	0.14 ± 0.01	0.20 ± 0.01	0.19 ± 0.01	0.17 ± 0.01	0.16 ± 0.01	0.20 ± 0.01	0.23 ± 0.02	0.26 ± 0.01	0.26 ± 0.02	0.28 ± 0.02
		0.11 ± 0.01	0.11 ± 0.01	0.12 ± 0.01	0.15 ± 0.01	0.13 ± 0.01	0.13 ± 0.01	0.14 ± 0.02	0.17 ± 0.02	0.08 ± 0.01	0.08 ± 0.00	0.09 ± 0.01
Force	**[mN]**	0.090 ± 0.007	0.085 ± 0.006	0.121 ± 0.005	0.115 ± 0.007	0.103 ± 0.008	0.096 ± 0.006	0.123 ± 0.008	0.138 ± 0.009	0.156 ± 0.009	0.156 ± 0.014	0.165 ± 0.012
		0.103 ± 0.009	0.101 ± 0.009	0.113 ± 0.011	0.147 ± 0.012	0.135 ± 0.010	0.251 ± 0.027	0.274 ± 0.037	0.415 ± 0.040	0.447 ± 0.034	0.526 ± 0.030	0.612 ± 0.046
Shortening	**[%]**	2.65 ± 0.19	2.53 ± 0.19	3.61 ± 0.19	3.51 ± 0.19	3.23 ± 0.23	3.15 ± 0.19	3.87 ± 0.25	4.33 ± 0.29	4.88 ± 0.23	4.86 ± 0.43	5.26 ± 0.39
		2.03 ± 0.17	2.00 ± 0.17	2.22 ± 0.20	2.67 ± 0.20	2.49 ± 0.16	2.40 ± 0.24	2.52 ± 0.32	2.98 ± 0.27	1.51 ± 0.10	1.50 ± 0.09	1.70 ± 0.12
Force Production Rate	**[mN/mm]**	1.77 ± 0.13	1.55 ± 0.11	2.30 ± 0.13	2.24 ± 0.13	2.15 ± 0.16	2.18 ± 0.14	2.56 ± 0.17	2.85 ± 0.20	3.17 ± 0.18	3.28 ± 0.29	3.31 ± 0.23
		2.02 ± 0.17	1.92 ± 0.16	2.22 ± 0.22	2.91 ± 0.21	4.14 ± 0.28	5.70 ± 0.61	6.98 ± 0.88	11.85 ± 1.12	9.38 ± 0.57	11.33 ± 0.59	12.20 ± 0.85
Force Relaxation Rate	**[mN/mm]**	1.47 ± 0.11	1.25 ± 0.09	1.93 ± 0.10	1.92 ± 0.12	1.85 ± 0.15	1.98 ± 0.15	2.15 ± 0.15	2.37 ± 0.18	2.67 ± 0.16	2.68 ± 0.27	2.85 ± 0.22
		1.74 ± 0.13	1.60 ± 0.12	1.92 ± 0.17	2.37 ± 0.18	3.52 ± 0.23	4.84 ± 0.49	5.72 ± 0.68	9.41 ± 0.88	7.52 ± 0.35	9.62 ± 0.44	10.01 ± 0.65
Contraction Velocity	**[mm/s]**	2.95 ± 0.22	2.59 ± 0.19	3.83 ± 0.22	3.73 ± 0.22	3.58 ± 0.27	3.64 ± 0.23	4.26 ± 0.28	4.74 ± 0.33	5.28 ± 0.30	5.47 ± 0.49	5.51 ± 0.38
		2.22 ± 0.18	2.11 ± 0.18	2.44 ± 0.24	2.90 ± 0.21	2.76 ± 0.19	2.85 ± 0.30	2.79 ± 0.35	3.38 ± 0.32	1.71 ± 0.10	1.65 ± 0.09	1.78 ± 0.12
Relaxation Velocity	**[mm/s]**	2.45 ± 0.18	2.09 ± 0.14	3.22 ± 0.16	3.19 ± 0.21	3.09 ± 0.25	3.30 ± 0.25	3.58 ± 0.26	3.94 ± 0.31	4.46 ± 0.27	4.47 ± 0.44	4.76 ± 0.37
		1.91 ± 0.14	1.76 ± 0.14	2.11 ± 0.19	2.36 ± 0.18	2.35 ± 0.15	2.42 ± 0.24	2.29 ± 0.27	2.69 ± 0.25	1.37 ± 0.06	1.40 ± 0.06	1.46 ± 0.09
Work	**[nJ]**	1.97 ± 0.16	1.85 ± 0.12	2.60 ± 0.10	2.44 ± 0.15	1.85 ± 0.12	2.07 ± 0.12	1.85 ± 0.12	2.89 ± 0.20	3.21 ± 0.19	3.28 ± 0.29	3.58 ± 0.26
		2.33 ± 0.18	2.27 ± 0.18	2.60 ± 0.23	3.18 ± 0.24	4.37 ± 0.32	5.50 ± 0.56	7.43 ± 0.95	8.73 ± 1.05	9.79 ± 0.86	12.10 ± 0.70	13.42 ± 1.09
Frequency	**[bpm]**	189 ± 26	143 ± 12	170 ± 21	255 ± 17	243 ± 16	276 ± 21	192 ± 16	194 ± 18	166 ± 20	150 ± 17	194 ± 32
		194 ± 22	167 ± 14	201 ± 25	232 ± 24	211 ± 15	256 ± 25	163 ± 12	185 ± 23	143 ± 15	153 ± 16	135 ± 21

Supplementary Table S2.

Table. S2. Calculation of gestational systolic wall stress: Literature values[23-26] of end-systolic left ventricular transverse diameter, longitudinal diameter, pressure, and wall thickness, used to calculate gestational circumferential wall stress in humans from 16 to 40 weeks of gestation. To obtain an estimate of the apparent stresses directly perceived by cardiomyocytes, wall stresses were multiplied by a factor of 1.25 (assuming a cardiomyocyte volume fraction of 80% within the left ventricle).

GW	Transverse Diameter (mm)	Longitudinal Diameter (mm)	Wall Thickness (mm)	Pressure (mm Hg)	Wall stress (mm Hg)	Wall Stress (mN/mm^2)	Cardiac Stress (mN/mm^2)
16	3.00	2.85	1.97	16.67	8.41	1.12	1.40
17	3.45	3.28	2.15	18.33	9.34	1.25	1.56
18	3.89	3.70	2.33	20.00	10.26	1.37	1.71
19	4.32	4.11	2.50	21.67	11.16	1.49	1.86
20	4.74	4.51	2.68	23.33	12.06	1.61	2.01
22	5.57	5.29	3.04	26.67	13.84	1.84	2.31
23	5.96	5.67	3.22	28.33	14.72	1.96	2.45
27	7.48	7.10	3.93	33.82	17.61	2.35	2.93
28	7.83	7.44	4.11	34.69	18.07	2.41	3.01
30	8.52	8.10	4.47	36.43	18.97	2.53	3.16
32	9.18	8.72	4.83	38.17	19.88	2.65	3.31
34	9.81	9.32	5.19	39.91	20.77	2.77	3.46
36	10.40	9.88	5.54	41.65	21.66	2.89	3.61
38	10.96	10.41	5.90	43.39	22.54	3.01	3.76
40	11.48	10.91	6.26	45.13	23.42	3.12	3.90